تأثير محتوى الكبريتات على الخواص السطحية لحفازات أكسيد القصدير (IV) المدعم بالكبريتات

حسين عبدالفتاح خلف، صابر السيد منصور، إيناس عبد المولي المدني

قسم الكيمياء، كلية العلوم، جامعة عمر المختار، البيضاء ص ب 919 ، ليبيا

الملخص:

في هذه الدراسة تم تحضير حفازات أكسيد القصدير النقية عن طريق إضافة محلول الأمونيا المخفف إلى محلول كلوريد (IV) القصدير حتى الوصول إلى رقم هيدروجيني 8.0 . وبعد غسيل الراسب المتكون عدة مرات والحصول على أكسيد القصدير (جل) وحرقه عند 873 كلفن لمدة 3 ساعات، ثم إضافة حمض الكبريتيك ½ مولاري إلى محلول الجل المتكون قبل عملية الحرق للحصول على حفازات أسيد القصدير المدعم بالكبريتات وبنسب مختلفة من الكبريتات (6، 12، 18 %). بعدها تم توصيف الحفازات بعدة تقنيات منها: التحليل الحراري الوزني والتفاضلي، حيود الأشعة السينية، إمتزاز النتروجين عند 77 كلفن، الأشعة تحت الحمراء باستخدام أقراص بروميد البوتاسيوم بالإضافة إلى قياس الحامضية عن طريق المعايرة الجهدية باستخدام بيوتيل الأمين العادي. وقد أظهرت النتائج أن الجل المتكون قبل الحرق يحتوي على جزيئين من الماء ($SnO2.2H2O$). كما أن إضافة الكبريتات لم تتسبب في حدوث تغيير لطور أكسيد القصدير (التركيب البلوري الرباعي) إلا أنها تسبب انخفاض في حجم الدقائق وبالتالي تحدث زيادة في مساحة السطح. وبزيادة محتوى الكبريتات تزداد كذلك مساحة السطح حتى تصل إلى 88م2/جم لعينة 18%. هذا بالإضافة إلى أن وجود الكبريتات على سطح الأكسيد تظهر تركيبين مختلفين من الكبريتات على السطح كما إتضح ذلك من فحص الأشعة تحت الحمراء. كما أن دراسة الحامضية قد أظهرت أن إضافة الكبريتات للأكسيد تسبب ظهور مراكز حامضية قوية جداً على السطح.

Journal of the Association of Arab Universities for Basic and Applied Sciences (2011) **10**, 15–20

University of Bahrain

Journal of the Association of Arab Universities for Basic and Applied Sciences

www.elsevier.com/locate/jaaubas
www.sciencedirect.com

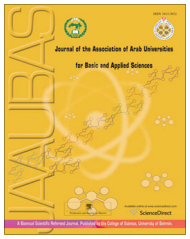

The influence of sulfate contents on the surface properties of sulfate-modified tin(IV) oxide catalysts

Hussein A. Khalaf *, Saber E. Mansour, Enas A. El-Madani

Chemistry Department, Faculty of Science, Omer El-Mukhtar University, P.O. 919, El-Beida, Libya

Available online 20 July 2011

KEYWORDS

Tin(IV) oxide;
Sulfation;
Acidity;
Texture

Abstract Tin(IV) oxide catalysts, pure and surface-doped with different loading levels of sulfate, have been prepared and characterized by means of thermal analysis (TGA and DTA), X-ray powder diffraction (XRD), nitrogen adsorption at 77 K, FT-IR spectroscopy using KBr pellets and potentiometric titration using *n*-butylamine. The catalysts were prepared from aqueous solutions of ammonia and tin(IV) chloride, with production of an amorphous precipitate that calcined at 873 K for 3 h to give tin(IV) oxide (SnO_2). The sulfation was carried out by impregnation of sulfuric acidic 0.5 M with tin(IV) hydroxide with different amounts of sulfate (6%, 12% and 18% SO_4^{-2} by weight). Structural investigation of the catalysts by TGA, XRD and N_2-sorption revealed that tin(IV) gel has at least two molecules of water to give the formula $SnO_2{\cdot}2H_2O$ and the addition of sulfate does not modify the crystalline structure of tin(IV) oxide (tetragonal phase) but decreases the crystallite size and, consequently, increase the specific surface area. The increase in loading level of sulfate resulted in increase in specific surface area of the catalysts. Acidity measurement by potentiometric titration using *n*-butylamine show that the addition of sulfate can increase the acidity of tin(IV) oxide and all sulfated tin(IV) oxide having strong acid sites. Moreover, FT-IR spectra expose that sulfated tin(IV) oxide has two different structures of sulfates.

1. Introduction

Tin(IV) oxide is an active catalyst for many reactions due to acidic, basic, oxidizing and reducing surface properties. It has become well established that the performance of a heterogeneous catalyst depends not only on the intrinsic catalytic activity of its components, but also on its texture and stability. One of the most important factors in controlling the surface properties of a catalyst involves the correct choice of the additives. The adsorption of various anions (Mekhemer, 2005), particularly sulfate or phosphate anions, onto oxide has been attempted as a means of improving their catalytic activity. The increase in activity is believed to arise from increase in the surface acidity of the modified oxide (Clearfield et al., 1994). Modification of metal oxides with sulfate anion can generate a strong acidity, even stronger than 100% sulfuric acid and hence they become superacid catalysts that are useful in reactions like isomerizations, low temperature esterification, alkylation and cracking (Jyothi1 et al., 2000; Song et al., 1996). Sulfated tin(IV) oxide is one of the candidates for

* Corresponding author.
E-mail address: hkhalaf70@yahoo.com (H.A. Khalaf).

Peer review under responsibility of University of Bahrain.
doi:10.1016/j.jaubas.2011.06.003

ELSEVIER **Production and hosting by Elsevier**

having the strongest acidity on the surface. The acid strength is reported to be higher than that of sulfated zirconia (El-Sharkawy et al., 2007; Hino et al., 2007). Ceramics acid of tungstated tin(IV) oxide prepared by Arata is more active than aluminosilicates for the esterification of *n*-octanoic acid with methanol (Hino et al., 2006). Other application of CO oxidation over SnO_2 and Pd/SnO_2 catalysts was reported by (Sasikala et al., 2000), whereas organic syntheses catalyzed by superacidic metal oxides: sulfated zirconia and related compounds were reviewed (Arata, 2009).

Nevertheless, papers concerning sulfated tin(IV) oxide catalyst have been quite few because of difficulty in preparation, compared with the easy preparation of other sulfated oxides. This study aimed to prepare tin(IV) oxide catalysts acidified with sulfate anions and study the effect of sulfate amounts on the surface properties of it. Tin(IV) oxide was prepared from stannic chloride and has been sulfated using sulfuric acid with different loading levels of sulfate (6%, 12% and 18% SO_4^{-2}). These sulfated catalysts were characterized using different tools to know the effect of sulfate levels on the surface properties of the SnO_2 catalysts.

2. Experimental

2.1. Materials

Tin(IV) oxide gel, used as a precursor of sulfated and promoted oxide, was prepared by the method described in the literatures (Matsuhashi et al.2001a,b). In brief, by a slow dropwise addition of a 1:1 aqueous ammonia to a 0.3 M aqueous solution of tin(IV) chloride ($SnCl_4{\cdot}5H_2O$) AR grade, BDH product (England), with a continuous stirring till pH = 8 is reached. The white precipitate was left over-night before being filtered and washed thoroughly with 2% CH_3COONH_4 solution until all chloride was eliminated (silver nitrate test), and then dried at 383 K till constant weight is obtained. The dried material was ground to 250 mesh size and kept dry over P_2O_5 desiccator. The dry gel thus obtained is denoted in the text as TH and it was used as a precursor for preparation of SnO_2 and modified SnO_2 catalysts. Pure tin oxide, SnO_2, was obtained from the dried gel (TH) by calcination at 873 K for 3 h. The resultant oxide, SnO_2 (XRD verified vide infra), was designated in the text as TO. Sulfated SnO_2 samples were prepared by impregnation of $SnO_2{\cdot}xH_2O$ (TH) gel with the appropriate amount of 0.5 M H_2SO_4 solution to obtain 6%, 12% and 18% SO_4^{-2} by weight. The resultant was dried at 383 K for 24 h, followed by calcination at 873 K for 3 h and the products were designated as *x*STO (where x = 6%, 12% and 18%).

2.2. Apparatus and techniques

2.2.1. Thermal analysis

Both TGA and DTA were performed between room temperature and 1273 K in a static atmosphere of air, using V2-2A DUPONT 9900 thermal analyzer. The rate of heating was standardized at 10 K min^{-1}, and small portions (5–15 mg) of the sample were used in TG measurements.

2.2.2. X-ray powder diffractometry

XRD diffractograms were recorded for all samples using a model JSX-60PA JEOL diffractometer (Tokyo, Japan) and CuKα radiation (λ = 1.5418 Å). The generator was operated at 35 kV and 20 mA. The samples were scanned in the range of 2θ = 10–70° at a scanning speed of 6 min^{-1}. For identification purposes, diffraction patterns (I/I°) versus d spacing (Å) were matched with the relevant ASTM standards (Frank, 1981). The crystallite size D of the samples were calculated using the Scherrer's relationship (Klug and Alexander, 1970):

$$D = \frac{k\lambda}{\beta \cos\theta} \quad (1)$$

where K is the crystallite shape constant ($\approx$1), λ the radiation wavelength, β the line breadth (radians) and θ is the Bragg angle.

2.2.3. Nitrogen sorption measurement

Full nitrogen adsorption/desorption isotherms at 77 K were obtained using a NOVA 2200 (version 6.10) high-speed gas sorption analyzer (Quantachrome Corp., Boynton Beach, FL, USA). The calcined samples were first outgassed at 470 K for 1 h. Twenty-four-point adsorption and desorption isotherms were obtained, from which BET surface areas were derived using standard and well-established methods (Sing et al., 1985; Webb and Orr, 1997).

2.2.4. FTIR measurement

A very small amount of finely ground solid sample (5–10 mg) is intimately mixed with powdered KBr (90 mg) and then pressed in a 7 mm die under high pressure. IR analyses of the catalysts were carried out over the frequency range of 4000–500 cm^{-1} using a Nicolet 380 FT-IR spectrophotometer with 4 cm^{-1} resolution.

2.2.5. Acidity measurement

The total acidity of the solid samples under investigation was measured by means of potentiometric titration (El-Sharkawy et al., 2007; Rao et al., 2006). The solid catalyst (0.1 g) was suspended in 10 ml acetonitrile (Merck), and agitated for 4 h. Then, the suspension was titrated with 0.1 N *n*-butylamine in acetonitrile at 0.10 ml min^{-1}. The electrode potential (Ei) variation was measured with SevenMulti, METTLER-TOLEDO, GMBH, Switerland. Cid and Pecci (1985) made a scale of acid strength measurement as follow: Ei > 100 mV for very strong sites; 0 < Ei < 100 mV for strong acid sites; −100 < Ei < 0 mV for weak sites; and finally Ei < −100 mV for very weak sites.

3. Results and discussion

3.1. Thermal analysis

From the TG profile of the precursor tin gel ($SnO_2{\cdot}xH_2O$), Fig. 1a, it can be seen that there are two mass loss steps in the temperature range RT-1273 K. The first step ends at 423 K with loss of mass ~3.6% and accompanied by an endothermic peak at 380 K, is attributed to the loss of volatile materials like physisorbed water (Magnacca et al., 2003). The second one begins just after the first (680 K) bringing the mass loss to ~19.9%, is assigned to dehydroxylation processes (DTA exothermic peak at 643 K) (Mekhemer et al., 2005; Wang and Xie, 2001). Theoretical mass loss of tin gel as stoichiometrically approaching $SnO_2{\cdot}2H_2O$ to anhydrous SnO_2 is 19.3% (Scheme 1). The experimental mass loss is

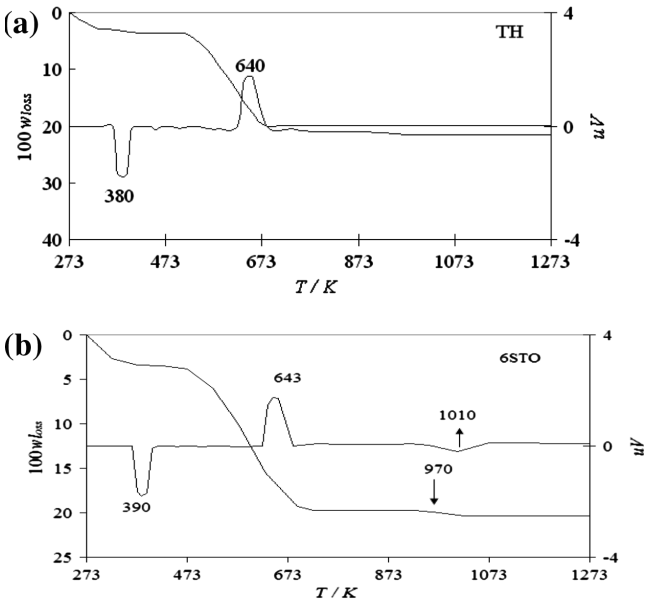

Figure 1 TGA and DTA profiles for (a) tin(IV) gel (TH), and (b) sulfated tin(IV) oxide (6STO), w_{loss} is the mass fraction.

$$SnO_2.2H_2O \xrightarrow{\triangle} SnO_2 + 2H_2O$$

Scheme 1

~19.9% hence this implies that the tin gel sample approaches the suggested formula. Therefore, the exhibited thermal events involve in general elimination of water of different strengths and a final formation of SnO_2, which agree with the XRD data. As to sulfated sample, 6STO, there are three mass loss steps, Fig. 1(b). The first two steps, ends at 473 K (endothermic peak at 393 K) and 643 K (exothermic peak at 693 K), are attributed to removal of adsorbed water and dehydroxylation process of tin gel. The mass loss at higher temperature began at 973 K and ended at 1053 K and accompanied by an endothermic peak at 1013 K, is attributed to decomposition of sulfate groups (Khalaf, 2009; Reddy et al., 2006).

3.2. X-ray diffraction

The XRD diffractograms of the sulfated samples with different loading levels of sulfate (6STO, 12STO and 18STO) calcined at 873 K are shown in Fig. 2. The main conclusion is that all patterns are characteristic of pure SnO_2 phase (ASTM card No. 41–1445) with tetragonal rutile structure at $2\theta = 26.54$, 33.82 and 51.74. The intensities of the bands characteristic for SnO_2 (TO) gradually decreased, while the width of the reflections is considerably broadened, indicating a small crystalline domain size (Khder et al., 2008). To know the role of sulfate content on the crystallinity of the samples quantitatively, their mean crystallite sizes were calculated from the broadening of the strongest peak of the samples and based on Scherrer equation (Table 1). The addition of sulfate was associated with a decrease in crystallite size to become 88, 50 and 31 Å for 6STO, 12STO and 18STO, respectively. This may be attributed to the sulfate groups that remain bounded at the surface of the

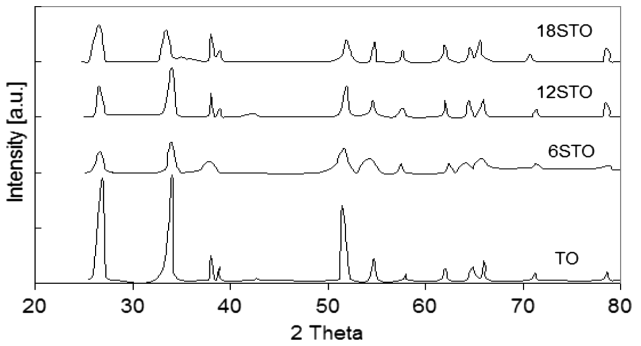

Figure 2 X-ray powder diffractograms for *x*STO in comparison with TO catalysts.

samples and inhibit the growth of SnO_2 crystallites, agreeing thus with the other transition metal oxides, i.e. TiO_2, ZrO_2 and Fe_2O_3 (Khder et al., 2008). The decrease in the crystallite size can be explained by the hypothesis that the bulky sulfate groups on the surface of SnO_2 particles prevent their agglomeration during calcination (Jogalekar et al., 1998).

3.3. Surface texture

The nitrogen sorption isotherms at 77 K of pure oxide (TO) and sulfated samples (6STO, 12STO and 18STO) were shown in Fig. 3. From this figure, it is clear that all isotherms are belonging to Type IV according to BET classification (Brunauer et al., 1938) and displays hysteresis loop of Type H3 mixed with some of H2 in case of 18STO sample according to the IUPAC classification (Sing et al., 1985). All the samples have a close closure point at $P/P_o = 0.4$. This may infer that the monolayer is completed slowly with contribution of micropores. The more pronounced knee on the adsorption isotherm of 6STO sample is reflected on its higher C_{BET} value (Table 1). This value greatly affects the shape of the isotherm in the low-pressure region whatever is the V_m value. Larger hysteresis loops can be noticed for TO, 6STO and 12STO samples.

Values of S_{BET}, S_t, V_P, r_P and C_{BET} for all samples are summarized in Table 1. It is apparent that S_{BET} and porosity are not similar for all samples, most likely due to variation in crystallite size. The good agreement between the S_{BET} and S_t values (Table 1) for all samples, reflects the higher accuracy of the BET-C determination and, consequently, the appropriateness of the reference Va-t curves (Gregg and Sing, 1982). From these data, it is clear that pure TO sample has low specific surface area ($S_{BET} = 11\ m^2\ g^{-1}$) which agrees with previous data (Harrison, 1989). The addition of su1fate into crystalline oxide resulted in a gradual increase in the surface area for the samples 6STO, 12STO and 18STO to become 35, 60 and 88 $m^2\ g^{-1}$, respectively. These data agree with the data obtained from XRD results, which complied in Table 1 also, in which the sulfated samples have small crystallite size (88, 50 and 31 Å for 6STO, 12STO and 18STO, respectively) that affect on the specific surface area (Khalaf, 2009).

The pore size distribution (PSD) curves for the samples, Fig. 4, show that the PSD lies between micropores and mesopores range. Three main peaks at < 20 Å were observed for all samples; in addition, some peaks were shown at radius higher than 20 Å. This means that the porosity of TO is

Table 1 Nitrogen sorption analysis data.

Sample	S_{BET} m^2g^{-1}	C_{BET}	S_t[a] m^2g^{-1}	S_S[b]	S_{cum}[c]	Vp_{cum}[d] cm^3g^{-1}	Vp_{tot}[e] cm^3g^{-1}	Aver r_P[f] Å	Crystallite size[g] (Å)
TO	11	14.7	10.3	10.8	6.9	0.016	0.0325	17.5	185
6STO	35	2.7	34	34.6	17.4	0.036	0.0387	18.5	88
12STO	60	3.5	59	58.8	19	0.035	0.048	13.5	50
18STO	88	4.0	87.7	86.5	41	0.066	0.1036	12.7	31

[a] The standard isotherm used in each case was selected according to (Sing et al., 1985).
[b] α_S Surface area.
[c] Cumulative surface area.
[d] Cumulative pore volume.
[e] Total pore volume at $P/P^o = 0.99$.
[f] Mean pore radius at the peak of the distribution curves.
[g] Obtained from XRD data.

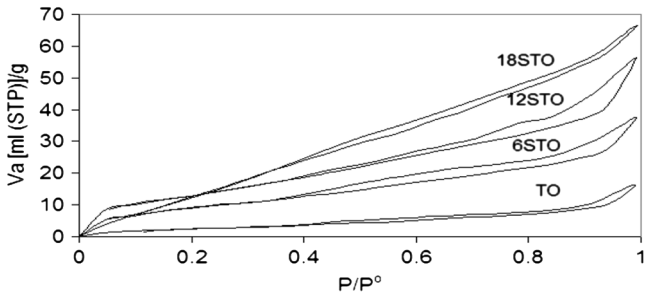

Figure 3 Nitrogen sorption isotherms for *x*STO in comparison with TO; V_a is measured at STP.

micropores in addition to little amount of mesopores. However, sulfated samples show a mix between mesopores and micropores in agreement with the findings of the *t*- and α_S-methods. Then, the incorporate of sulfates onto tin(IV) oxide can modify its porosity.

3.4. FTIR spectroscopy

Fig. 5 shows the IR spectra of sulfated tin(IV) oxide (*x*STO) in comparison with pure tin(IV) oxide (TO). From these spectra, the presence of sulfate groups was confirmed by the bands at 1382, 1190, 1155 and 1079 cm^{-1}. The first band (at 1382 cm^{-1}) characteristic of the surface sulfate species having S═O covalent bonds (Mekhemer et al., 2005). The other bands at 1190, 1155 and 1079 cm^{-1} are due to the asymmetric and symmetric stretching frequency of the O═S═O and O–S–O group (Mekhemer et al., 2005; Clearfield et al., 1994). Thus, it is evident that the IR spectra of both types of sulfated samples show very similar spectral features in the SO stretching region. These features are in general attributed to triply bridging sulfate and bridged bidentate sulfate, as represented in structures (I) and

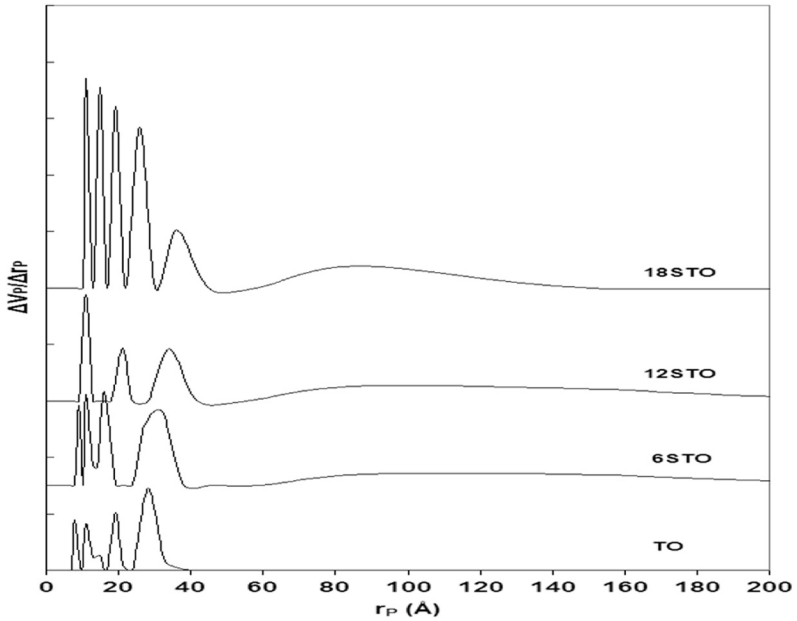

Figure 4 Pore size distribution curves for *x*STO in comparison with TO catalysts; r_p true radius and $\Delta V_P \cdot \Delta r_P^{-1}/cm^3\ g^{-1}\ Å^{-1}$ is the ratio between the volume decrease (ΔV_P) in $cm^3\ g^{-1}$ and the decrease in pore radius (Δr_p^{-1}) in $Å^{-1}$.

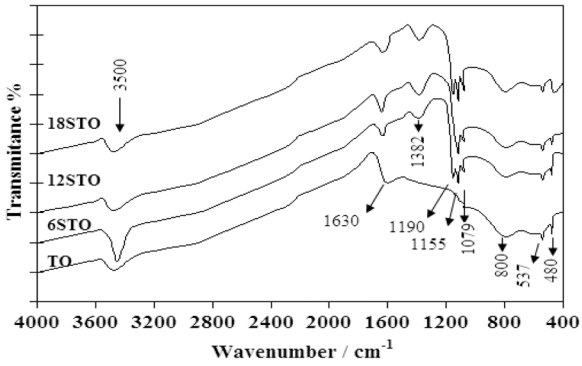

Figure 5 FTIR spectra for *x*STO in comparison with TO catalysts.

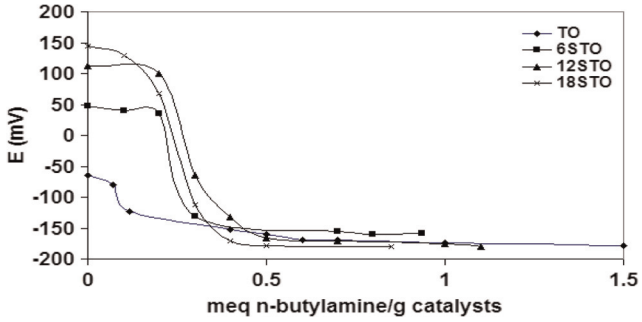

Figure 6 Potentiometric titration curves for *x*STO in comparison with TO catalysts; E is the electrode potential (mV).

(II) where M is Sn ion (Jin et al., 1986; Bensitel et al., 1988). The only effect of sulfate loading resulted in increase in the band intensities of sulfate group.

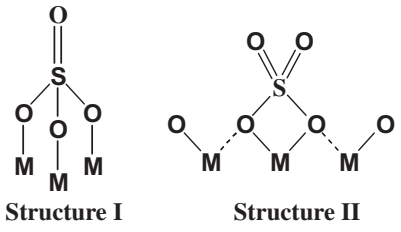

3.5. Acidity of the catalysts

Total number of acid sites and their relative strength, for the catalysts under investigation, can be measured by means of a potentiometric titration with 0.1 N *n*-butylamine. To explain the obtained results, it was suggested that the initial electrode potentional (Ei) indicates the maximum acid strength of the sites. The value of meq amine/g solid, where the plateau is reached in titration curves (Fig. 6), indicates the total number of acid sites (El-Sharkawy et al., 2007; Cid and Pecci, 1985). Table 2 shows the potentiometric titration results for all samples. From these results one can conclude that the TO sample has weak acid sites and its maximum strength is equal −65 mV. The addition of sulfate to SnO_2 can increase the acidic strength and create strong and very strong acid sites on the surface of SnO_2 to become +47, 112 and 144 mV for the samples 6STO, 12STO and 18STO, respectively.

Table 2 Potentiometric titration data for the catalysts.

Sample	Ei (mV) = maximum acid strength	No of acid sites (meq g^{-1})
TO	−65	0.11
6STO	+47	0.30
12STO	+112	0.40
18STO	+144	0.40

4. Conclusion

The obtained results show that the SnO_2 gel has at least two molecules of water to give the formula $SnO_2{\cdot}2H_2O$ and the addition of sulfate has no effect on the crystalline phase of SnO_2 (tetragonal phase) but decreases the crystallite size and, consequently, increase the specific surface area. The specific surface area is increased by increasing the loading of sulfate. FT-IR spectra expose that sulfated SnO_2 has two different structures of sulfates. Moreover, the incorporation of sulfate onto SnO_2 can increase its acidity and creates strong acidic sites.

References

Arata, K., 2009. Green Chemistry (RSC) 11, 1719–1728.
Bensitel, M., Saur, O., Lavalley, J.C., Morrow, B.A., 1988. An infrared study of sulfated zirconia. Mater. Chem. Phys. 19, 147–156.
Brunauer, S., Emmett, P.H., Teller, T., 1938. Adsorption of gases in multimolecular layers. J. Am. Chem. Soc. 60, 309–319.
Cid, R., Pecci, G., 1985. Potentiometric method for determining the number and relative strength of acid sites in colored catalysts. J. Appl. Catal. A: Gen. 14, 15–21.
Clearfield, A., Serrette, G.P.D., Khazi-Syed, A.H., 1994. Nature of hydrous zirconia and sulfated hydrous zirconia. Catal. Tod. 20, 295–312.
El-Sharkawy, E.A., Khder, A.S., Ahmed, A.I., 2007. Structural characterization and catalytic activity of molybdenum oxide supported zirconia catalysts. Micropor. Mesopor. Mater. 102, 128–137.
Frank, W. et al. (Eds.), 1981. Powder Diffraction File for Inorganic Phase. International Center for Diffraction Data, Philadelphia.
Gregg, S.J., Sing, K.S.W., 1982. Adsorption, Surface area and Porosity, 2nd edn. Academic Press, London.
Harrison, P.G., 1989. Chemistry of Tin. Blackie, Glasgow (Chapter 12).
Hino, M., Takasaki, S., Furuta, S., Matuhashi, H., Arata, K., 2007. Meta-Stannic acid as an effective support for the preparation of sulfated and tungstated stannias. Appl. Catalysis A General 321 (2), 147–154.
Hino, M., Takasaki, S., Furuta, S., Matsuhashi, H., Arata, K., 2006. Synthesis of a ceramics acid of tungstated stannia more active than aluminosilicates for the esterification of *n*-octanoic acid with methanol. Catalysis Comm. 7, 162–165.
Jin, T., Yamaguchi, T., Tanabe, K., 1986. Mechanism of acidity generation on sulfur-promoted metal oxides. J. Phys. Chem. 90, 4794–4796.

Jogalekar, A.Y., Jaiswal, R.G., Jayaram, R.V., 1998. Activity of modified SnO_2 catalysts for acid-catalysed reactions. J. Chem. Technol. Biotechnol. 71, 234–240.

Jyothi, T.M., Sreekumar, K., Talawar, M.B., Mirajkar, S.P., Raol, B.S., Sugunan, S., 2000. Physico-chemical characteristic of sulfated mixed oxides of Sn with some rare earth elements. Polish J. Chem. 74, 801–812.

Khalaf, H.A., 2009. Textural properties of sulfated iron hydroxide promoted with Al. Monatsh. Chem. 140, 669.

Khder, A.S., El-Sharkawy, E.A., El-Hakam, S.A., Ahmed, A.I., 2008. Surface characterization and catalytic activity of sulfated stannia catalyst. Catal. Commun. 9, 769–777.

Klug, H.P., Alexander, L.E., 1970. X-ray diffraction procedures. Wiley, New York, p. 490 (Chapter 9).

Magnacca, G., Cerrato, G., Morterra, C., Signoretto, M., Somma, F., Pinna, F., 2003. Structural and surface characterization of pure and sulfated iron oxides. Chem. Mater. 15, 675–687.

Matsuhashi, H., Miyazaki, H., Arata, K., 2001a. The preparation of solid superacid of sulfated stannia with acidity higher than sulfated zirconia. Chem. Lett. 452.

Matsuhashi, H., Miyazaki, H., Kawamura, Y., Nakamura, H., Arata, K., 2001b. Preparation of a solid superacid of sulfated stannia with acidity higher than that of sulfated zirconia and its applications to aldol condensation and benzoylation. Chem. Mater. 13, 3038–3042.

Mekhemer, G.A.H., 2005. Surface characterization of zirconia, holmium oxide/zirconia and sulfated zirconia catalysts. Colloids and Surfaces A: Physicochem. Eng. Aspects 274, 211–218.

Mekhemer, G.A.H., Khalaf, H.A., Mansour, S.A.A., Nohman, A.K.H., 2005. Sulfated alumina catalysts: consequences of sulfate content and source. Monatsh. Chem. 136, 2007–2016.

Rao, K.N., Reddy, K.M., Lingaiah, N., Suryanarayana, I., Prasad, P.S., 2006. Structure and reactivity of zirconium oxide-supported ammonium salt of 12-molybdophosphoric acid catalysts. J. Appl. Catal. A: Gen. 300, 139–146.

Reddy, B.M., Sreekanth, P.M., Lakshmanan, P., Khan, A., 2006. Synthesis, characterization and activity study of $SO_4^{-2}/Ce_xZr_{1-x}O_2$ solid superacid catalyst. J. Mol. Catal. A: Chem. 244, 1–7.

Sasikala, R., Gupta, N.M., Kulshreshtha, S.K., 2000. Temperature-programmed reduction and CO oxidation studies over Ce–Sn mixed oxides. Catal. Lett. 71, 69–73.

Sing, K.S.W., Everett, D.H., Haul, R.A.W., Moscou, L., Pierotti, R.A., Rouquerol, J., Siemieniewska, T., 1984. Reporting physisorption data for gas/solid systems with special reference to the determination of surface area, porosity (Recommendations 1984). Pure Appl. Chem. 57, 603.

Song, X., Reddy, K.R., Sayari, A., 1996. Effect of Pt and H_2Onn-butane isomerization over Fe and Mn promoted sulfated zirconia. J. Catal. 161, 206–210.

Wang, X., Xie, Y., 2001. Low-temperature ch_4 total oxidation on catalysts based on high surface area SnO_2. React. Kinet. Catal. Lett. 72, 115.

Webb P.A., Orr C. (1997). Analytical Methods in Fine Particle Technology, Micromeretics, Norcross, GA, USA. Chapter 1–4.